NASA High-Reynolds Number Circulation Control Research - Overview of CFD and Planned Experiments (Invited)

W. E. Milholen II*, G.S. Jones†, and C.M. Cagle‡
NASA Langley Research Center, Hampton, VA, 23681-2199

A new capability to test active flow control concepts and propulsion simulations at high Reynolds numbers in the National Transonic Facility at the NASA Langley Research Center is being developed. This technique is focused on the use of semi-span models due to their increased model size and relative ease of routing high-pressure air to the model. A new dual flow-path high-pressure air delivery station has been designed, along with a new high performance transonic semi-span wing model. The modular wind tunnel model is designed for testing circulation control concepts at both transonic cruise and low-speed high-lift conditions. The ability of the model to test other active flow control techniques will be highlighted. In addition, a new higher capacity semi-span force and moment wind tunnel balance has been completed and calibrated to enable testing at transonic conditions.

Nomenclature

c	= local airfoil chord
C_D	= drag coefficient
C_L	= lift coefficient
C_l	= sectional lift coefficient
C_m	= airfoil pitching moment
C_p	= surface pressure coefficient
C_μ	$= \dot{m}U_j / q_\infty S$
h	= blowing slot height
M	= local value of Mach number
M_{DD}	= drag divergent value of freestream Mach number
M_∞	= freestream Mach number
$\dot{m}$	= mass flow, lbm/sec
NPR	= nozzle pressure ratio, p_{oj} / p_∞
p	= pressure
q_∞	= freestream dynamic pressure
Re	= Reynolds number based on mean aerodynamic chord
S	= wing reference area
T	= temperature
U_j	= total velocity at jet exit
u,v,w	= velocity components in the x,y,z directions
x,y,z	= Cartesian coordinate system
α	= angle-of-attack, degrees
η	= non-dimensional semi-span location

subscripts

j	= jet exit location
o	= stagnation quantity
∞	= freestream quantity

---

* Research Engineer, Configuration Aerodynamics Branch, MS 499, Senior Member AIAA.

† Research Engineer, Flow Physics and Control Branch, MS 170, Senior Member AIAA.

‡ Design Engineer, Aeronautics Systems Engineering Branch, MS 238.

I. Introduction

Active flow control continues to be a fertile research field that holds promise to enhance the aerodynamic performance of conventional aircraft and enable the development of unconventional vehicles. A wide variety of active flow control techniques are being pursued, ranging from direct boundary layer manipulation using steady or pulsed blowing methodologies, to indirect methods including induced plasma flows near a surface[1]. Computational Fluid Dynamic (CFD) methods are maturing to the point that they are being used as tools to improve and optimize flow control techniques on realistic configurations. The confidence in these CFD tools can be improved as they are systematically validated. In general, CFD validation is defined by determining how well the CFD model predicts the performance and flow physics when used for its intended purposes[2,3]. The level of CFD validation can be defined by the complexity of the code and the experiment being used for validation, as described in Figure 1.

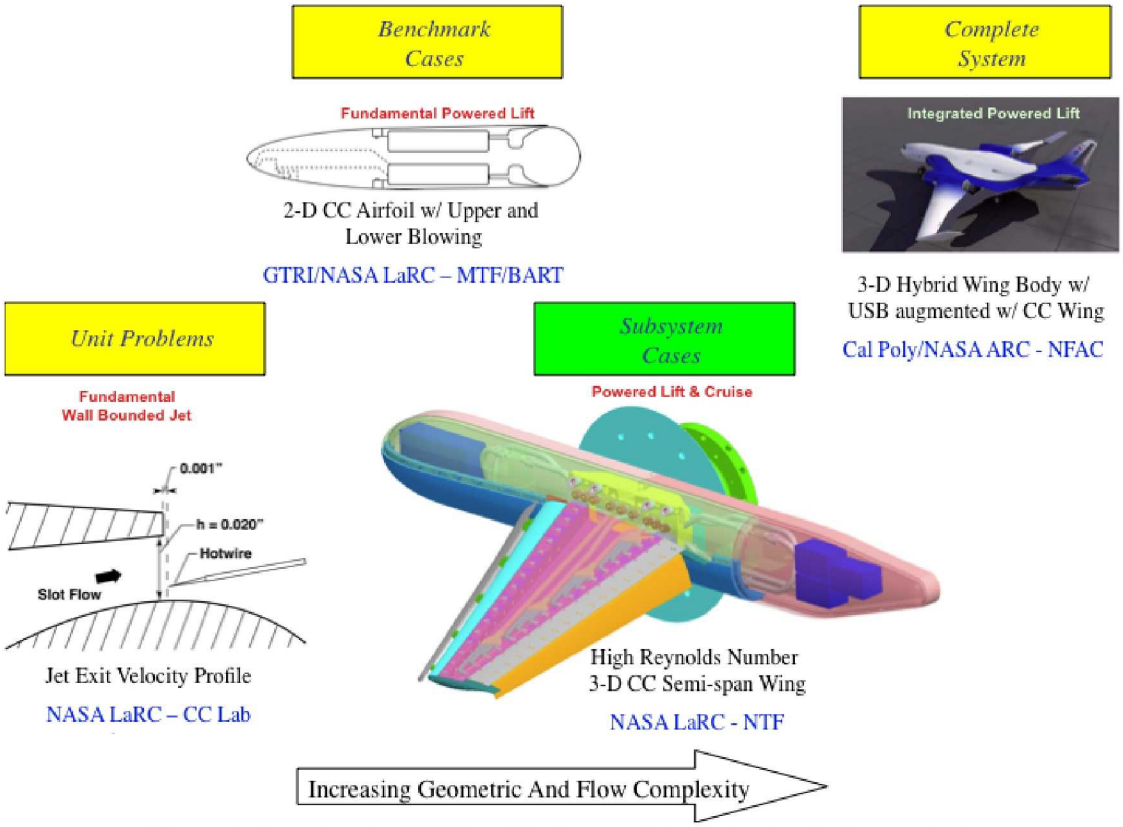

Figure 1. Four levels of CFD validation used to study circulation control.

One active flow control technique that has experienced a resurgence in research is circulation control[4,5,6,7,8,9]. The circulation control method introduces momentum directly to the near wall region via a blowing slot, typically located near the trailing edge and directed over a simple short-cord flap as shown in Figure 2. The resulting simplified high-lift system can generate maximum lift values significantly higher than that of a conventional multi-element high-lift system. The introduced high momentum flow from the blowing slot is typically characterized by the non-dimensional blowing coefficient (C_μ), and the ratio of the slot height to local wing chord (h/c), and the Nozzle Pressure Ratio (NPR). On an aircraft, one supply option for the circulation control system is engine bleed air, which was shown to be viable by a recent e-STOL aircraft design study[10]. It is worthy to note that unsteady circulation control methods are also being examined to reduce the bleed air requirements. Another advantage, which has yet to be fully addressed, is the

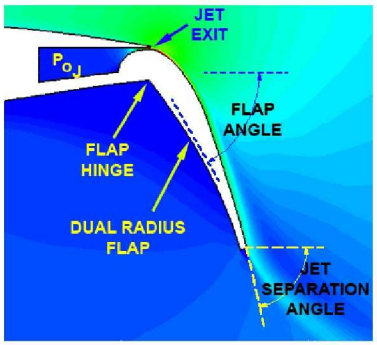

Figure 2. Circulation control blowing slot arrangement in the flap trailing edge region.

application of the circulation control technique during transonic cruise[11] for either drag reduction or for simplified maneuvering systems.

Several recent publications[12,13,14,15,16] have begun to highlight the developing database that can be used for CFD validation. As with most publically available active flow control datasets, one shortfall that still remains is the lack of data at realistic Reynolds numbers and data for Reynolds number effects, thereby limiting the scalability of the flow control techniques to flight conditions. To address this overarching need, a research project was begun to develop the capability to test active flow control concepts and propulsion simulations at high Reynolds numbers in the National Transonic Facility (NTF) at the NASA Langley Research Center.

The new flow control and propulsion simulation capability at the NTF is focused on the use of semi-span models due to the relative ease of routing high-pressure air to the model, and the increased model size compared to a conventional sting mounted full-span model. The increased model size allows higher model fidelity, as well as increased internal volume for housing the flow control mechanisms and instrumentation. A new high-pressure air delivery station has been designed which has a "low" mass flow segment for flow control simulations, and a "high" mass flow segment for propulsion simulations. Two new wind tunnel models are being developed for the initial testing with this air station. The first is a simple model which employs two check-standard nozzles to verify the operational characteristics of the air station. The second model is a high-performance transonic wing that will be used to evaluate various circulation control concepts at *both* transonic cruise conditions, as well as low-speed high-lift conditions. Lastly, a new higher load capacity semi-span force and moment balance has been completed and calibrated for the transonic testing. This paper will give an overview of all three aspects needed to develop the new high Reynolds number flow control and propulsion simulation testing capability at the NTF. In addition, the modular design employed for the new transonic semi-span model will be emphasized, as it can readily be re-configured for testing other flow control techniques.

II. Results and Discussion

A. Wind Tunnel Air Station Design

The NTF air station utilizes a dual flow air delivery system that is coupled to the NTF Sidewall Mounted Support System (SMSS) as depicted in Figure 3. The two independently controlled airlines pass through the center of the force and moment balance and couple to the model using two concentric bellows and the model interface plate as shown in Figure 4. The high flow line can provide 0.1-20.0 lbm/sec and the low flow line delivers 0.1-8.0 lbm/sec to the model.

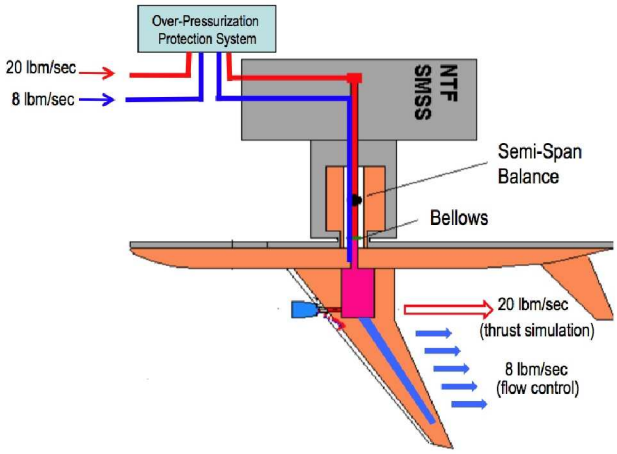

Figure 3. Schematic diagram of the routing of high-pressure air to a semi-span mounted on the sidewall of the NTF for flow control and propulsion simulation testing.

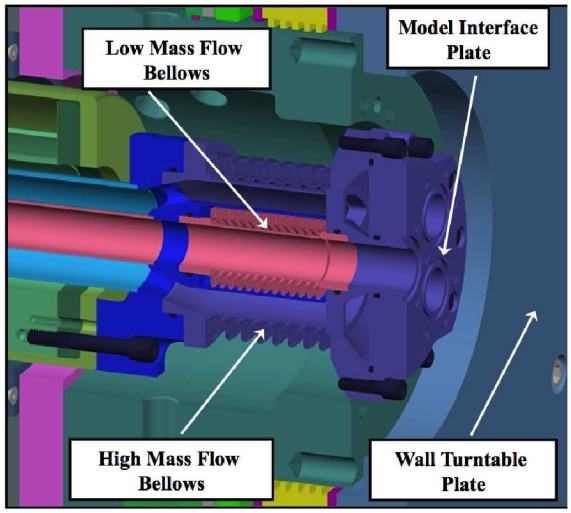

Figure 4. Cross sectional view of the bellows arrangement at the wind tunnel model attachment location.

The external high-pressure air system provides a continuous flow of clean, dry air to the SMSS. Initial operations of the facility will be limited to total pressure of 5 atmospheres and a total temperature of -50 °F when the air station is being used to avoid the formation of frost in the tunnel circuit[17]. The air station provides pre-heated high-pressure air to the model, thus low temperature control of the jet is obtained through Joule Thompson effects and heat transfer through conduction of the pipes that are exposed to the cold temperatures inside the facility plenum (-50 °F< T_o <120 °F).

As part of the air delivery system a fast acting model protection system was added to enable various model designs. Internal flow paths are often manipulated with choke plates, valves, or flow straighteners. These devices can create large pressure requirements that are unique to a given wind tunnel model. The isolation and vent system can be adjusted for maximum internal pressures that vary from 400 – 1200 psig to match the design pressure limits of the given wind tunnel model. In the event of a pressure spike, the model over-pressure protection system would automatically isolate and vent the wind tunnel model, and command a shut down and venting of the high-pressure air delivery system. The design requirement for the isolation and venting of the wind tunnel model was a reaction time of one second or less. The ventilation valves can also be used to pre-condition the air temperature of the system, efficiently allowing this procedure to occur while the wind tunnel is being brought onto condition.

B. Wind Tunnel Air Station Validation

To verify the air station test envelope, it is essential to size the nozzles and internal choke plates for the highest mass flow rate and internal pressures. An additional benefit of the air station evaluation is the characterization of the "air on" model and air station interface. This model uses readily available Stratford calibration nozzles[18] from the NASA inventory that have known thrust characteristics. The initial nozzles selected are based on near term jet areas associated with Circulation Control and Propulsion Airframe Integration.

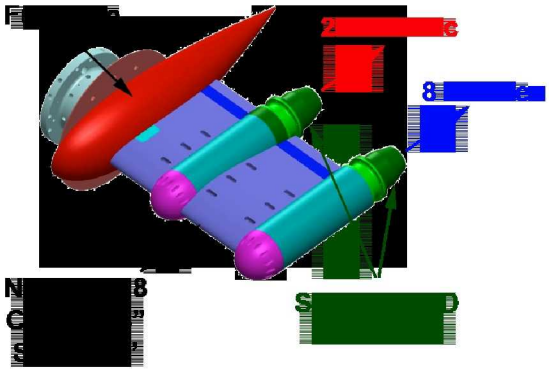

Figure 5. Conceptual sketch of dual nozzle check standard configuration for air station performance validation.

The maximum flow rate for either leg occurs at the lowest free stream Mach number and highest free stream static pressure as shown in figure 6. The internal model pressure is limited to 1200 psig and is based on the high-pressure limit of the air station piping system. The maximum mass flow rate for the high mass flow leg is 20 lbm/sec. With the wind tunnel pressurized to 5 ATM the NPR limit varies from 1.85 to 2.2 for jet temperatures

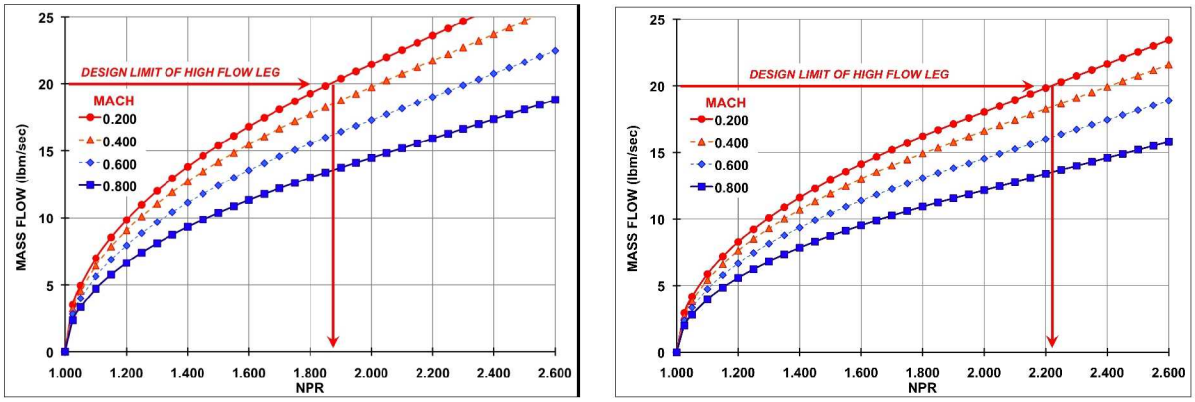

a) $T_o = T_{o,j}$=-50°F b) $T_o = T_{o,j}$=120°F

Figure 6. Mass characteristics for high mass flow nozzle (p_o= 5 ATM, Diameter: 2.7 inches).

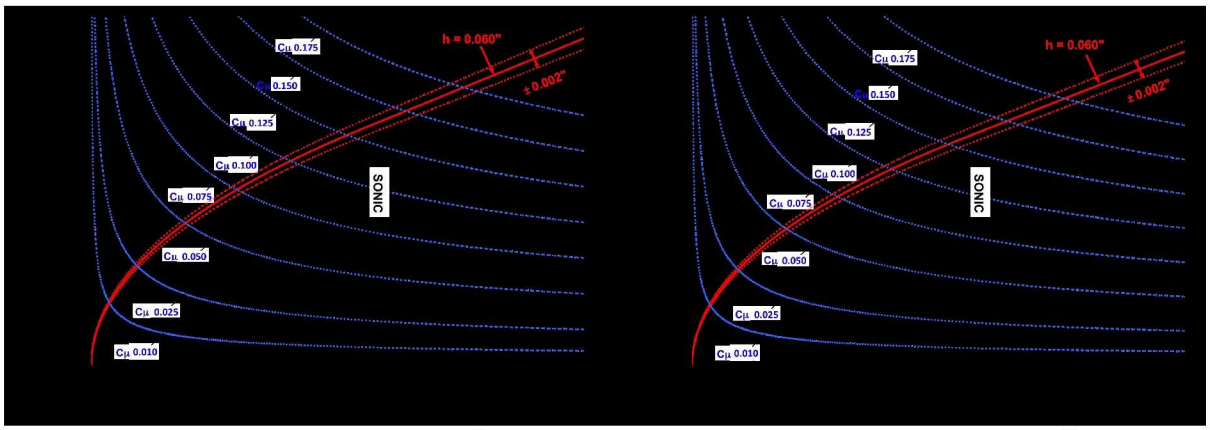

a) p_o=5 ATM, $T_o = T_{o,j}$=-50°F b) p_o=1 ATM, $T_o = T_{o,j}$=120°F

Figure 7. Mass flow characteristics for typical circulation control wing(h/c=0.0033, Slot Area=2.64 in^2).

that range from -50°F to 120°F. The corresponding estimated thrust is 600 lbf. These estimates are based on a nozzle diameter of 2.7 inches, and are characteristic of the model scales to be tested in the NTF.

Nominally the pressure in the plenum just prior to the jet exit establishes the NPR. It is important that the losses across the internal flow path that distributes the flow through the nozzle or circulation control slot is accounted for. Many of these devices have minimal losses, but major losses through choke plates occur. The maximum predicted upstream choke plate pressure described above occurs at the higher temperature and is approximated to be 1000 psig for a 37% open choke plate. The model safety system can be adjusted to the maximum allowable internal pressure of the model or 1200 psig (whichever is lower).

The non-dimensional momentum coefficient, Cμ, is used to characterize the performance of the many of the active flow control methods such as circulation control. The experimental uncertainty of Cμ can be related to the uncertainty in the measurement of both the mass flow and the slot height. Figure 7 highlights only the sensitivity of accurate slot height measurements on the Cμ coefficient. It should be noted that the air station is staged with two flow meters per leg. The anticipated accuracy of each flow meter is 1% of reading, with the low limit being approximately 0.01 lbm/sec. The actual mass flow measurement accuracy will be evaluated during the initial testing with the check standard nozzles.

C. Transonic Wing Design

Figure 8 shows the planform of the new semi-span model. The wing has an aspect ratio of 5.0, taper ratio of 0.40, a leading edge sweep of 30°, and no dihedral. The chord length at the side of the fuselage is 25.0 inches, resulting in a mean aerodynamic chord of 18.1 inches. The circulation control blowing slot is located at the 85% chord location on the upper surface, and will be directed over a 15% chord simple hinged flap when the model is in the high-lift mode. The generic fuselage is comprised of elliptic cross sections with a maximum width of 4.0 inches. The wing is mounted in the mid-fuselage position to simplify the routing of the high-pressure air supply lines. For wind tunnel testing, the model will be offset from the tunnel sidewall using a 2.0-inch non-metric standoff [17], which has a profile shape identical to that of the fuselage centerline.

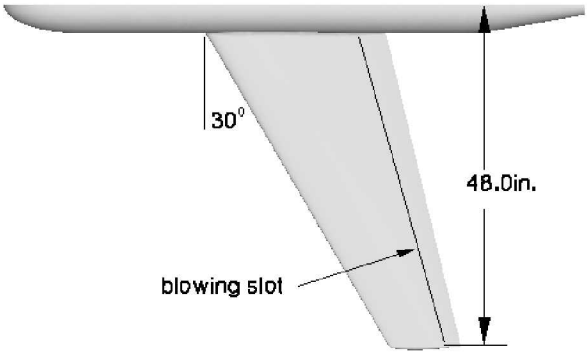

Figure 8: Planform view of NTF circulation control semi-span model.

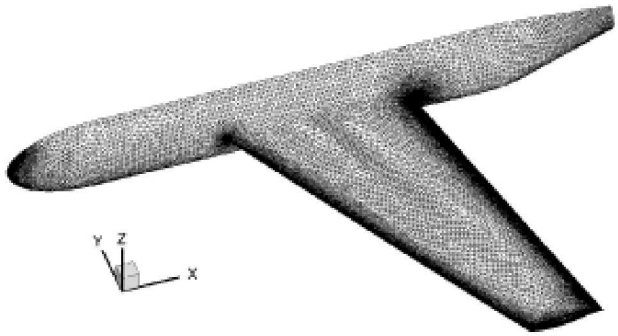

Figure 9. View of surface grid for transonic cruise configuration.

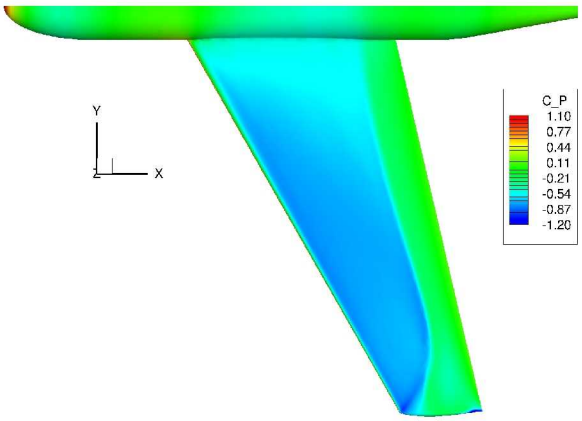

Figure 10: Predicted upper surface pressure contours (M=0.85, C_L = 0.50, Re = 30x10^6).

The wing was designed for a Mach number of 0.85, a lift coefficient of 0.50, at a Reynolds number based on mean aerodynamic chord of 30x10^6. The unstructured Navier-Stokes flow solver USM3D[19] was used in conjunction with the CDISC[20] design code. The CDISC design method is highly efficient because the geometry changes are introduced in a manner that allows both the geometry and the simulated aerodynamic analysis to converge in unison. The flow was assumed to be fully turbulent, and a wall-function version of the Spalart-Allmaras turbulence model was employed. The grid had approximately 5 million cells and was found to provide reasonably grid converged results. A partial view of the cruise grid is shown in Figure 9. It should be noted that the design and analysis was conducted simulating the configuration in "free-air", and the circulation control blowing slot was not included.

The initial wing loft utilized a modern supercritical airfoil section, the NASA TMA-0712[21]. The CDISC design method was used to improve the wing using several geometry and flow field constraints. The airfoil thickness to chord distribution on the outboard portion of the wing was decreased to 10%, while the original 12% thickness ratio was maintained over the inboard half of the wing. The final wing design has a weak shockwave that is shown in Figure 10, where the upper surface pressure coefficient contours are displayed. The wing has approximately 3° of washout, with a linear spanwise variation. A representative pressure distribution is shown in Figure 11 at η= 0.625. A state-of-the-art supercritical pressure distribution was achieved, with a weak shock wave located at approximately 75% chord. The wing performs well over a wide range of Mach number, which is highlighted in Figure 12 where the M(L/D) ratio is plotted at the design lift coefficient of 0.50.

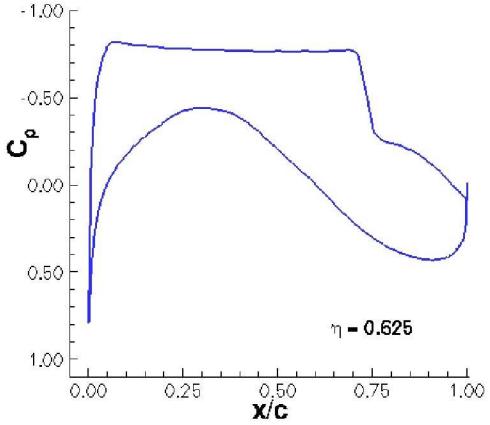

Figure 11. Predicted chordwise pressure distribution (M=0.85, C_L = 0.50, Re = 30x10^6).

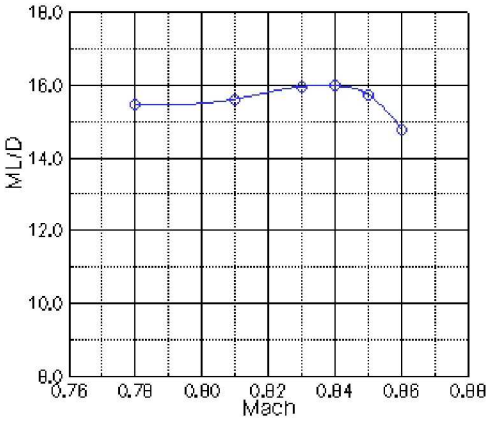

Figure 12. Effect of Mach number on aerodynamic performance (C_L = 0.50, Re = 30x10^6).

D. Low Speed High-Lift Design

The high-lift design effort focused on optimizing the leading edge slat position and the circulation control blowing slot utilizing a simplified flap geometry. A preliminary 2-D high-lift design study was performed on the NASA TMA-0712 airfoil to understand the influence of the circulation control blowing parameters. Figure 13 depicts the geometry, which has a 15% chord flap, deflected to 60°, and a blowing slot height of 0.003c. A 10% chord slat, deflected downward 30°, protects the leading edge of the airfoil from separation. The detailed view of the plenum region shows the vertical face upon which a resulting mass flow is introduced by specifying the static and stagnation pressures, analogous to setting the NPR. The CFD design study was conducted using USM3D in the "quasi 2-D" mode (eg. one cell wide grid), requiring approximately 370,000 cells. The Spalart-Allmaras turbulence model was again used, however in the full-viscous mode, with the y+ value for the 1st cell off the surface being approximately unity.

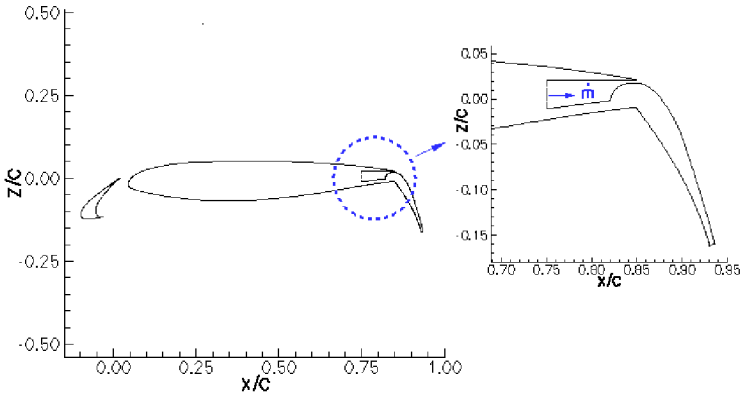

Figure 13. Two-dimensional high-lift circulation control airfoil geometry

The 2-D design study was successful in designing an effective slat in the presence of the actively blown trailing edge flap. The effect of the leading edge slat on the lift coefficient is shown in Figure 14, for NPR=1.60. Without the slat, the leading edge of the main element separates, yielding a maximum lift coefficient of 3.0 at zero degrees angle-of-attack. The slat increases the stall angle to 15°, with a maximum lift coefficient of approximately 5.70. It was noted that the flap remained attached through the entire angle-of-attack range, and stall occurred due to separation on the slat and main element. This comparison also indicates the performance benefits that a leading edge blowing slot[22] would need to attain to effectively replace the slat, which will be examined in the near future.

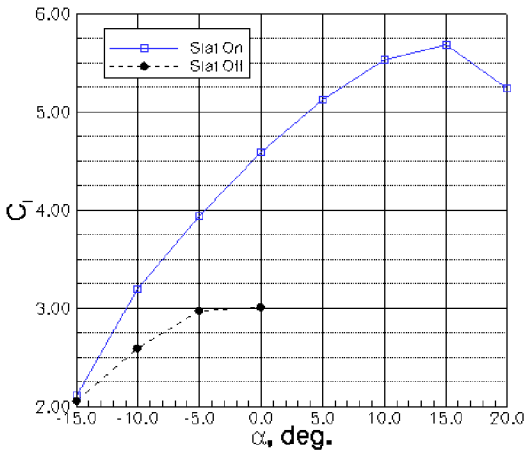

Figure 14. Effect of leading edge slat on 2-D high-lift circulation control airfoil (M=0.20, Re=20x10^6).

The high-lift system designed for the semi-span model is shown in Figure 15. Both the leading edge slat and the 15% chord trailing edge flap span the entire length of the wing. A streamwise slice through the wing at any spanwise location would be similar to the 2-D geometry shown in Figure 13. To simplify the construction of the wind tunnel model, the slat was designed to be a bolt-on addition to the cruise wing. Thus, the slat does *not* simulate the deployment of the cruise leading edge as would occur on an actual aircraft. This simplification does have an impact on the maximum obtainable lift coefficient. In the context of developing a versatile research configuration, this was however deemed an acceptable compromise.

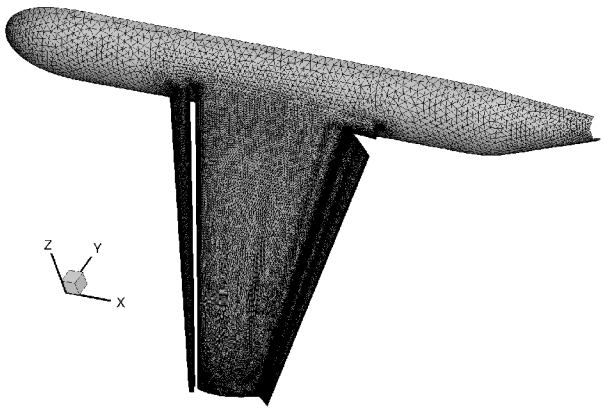

Figure 15. View of surface grid for high-lift configuration, 60° flap deflection.

The USM3D flow solver was used to conduct parametric studies that varied the trailing edge deflection angle, the blowing slot height, and the rigging of the leading edge slat. The full-viscous option was again utilized with the Spalart-Allmaras turbulence model, with the finest grid comprised of approximately 31 million cells, which was deemed adequate for the design effort. Only salient features of the high-lift design study will be presented.

Figure 16 demonstrates the effect of the aft plenum nozzle pressure ratio on the lift coefficient. With no blowing, NPR = 1.00, the simple hinged trailing edge flap experiences flow separation through the entire angle-of-attack range. The addition of blowing attaches the flow over the flap and provides a significant increase in lift. The lift increment due to blowing at zero degrees angle of attack is 1.45, for NPR=1.60. A further increase in the blowing to NPR=1.80 provides a nearly constant lift increment at all angles-of-attack. For this blowing rate, it was noted that the exit Mach number at the blowing slot is nearly sonic across the span of the wing. The predicted near surface streamline patterns at C_{Lmax} for the NPR=1.80 case are shown in Figure 17. The flow over the entire upper surface of the wing is attached, with the only appreciable spanwise flow occurring near the wing tip on the main element. This region becomes the locus of the wing stall as the angle-of-attack is further increased.

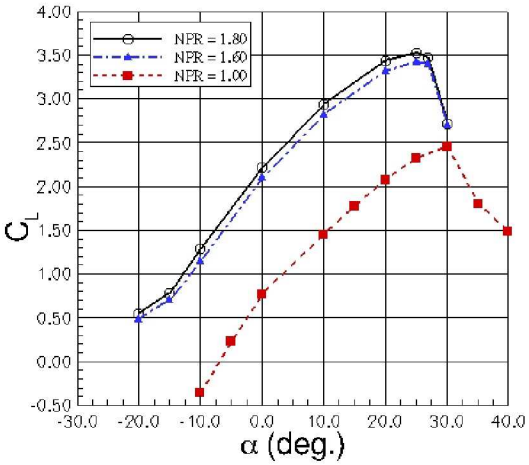

Figure 16. Effect of NPR on high-lift performance (M=0.20, Re = 20x10^6).

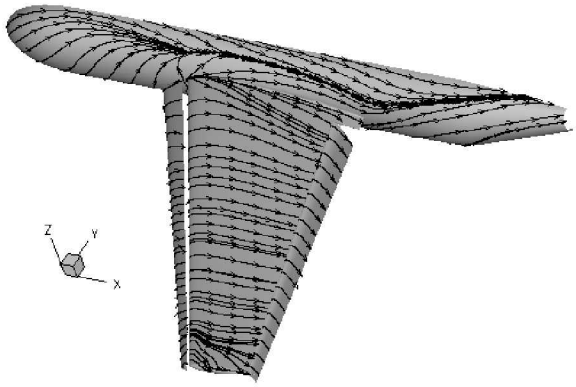

Figure 17. Predicted upper surface streamline patterns at C_{Lmax} for NPR=1.80 (M=0.20, α = 25°, Re = 20x10^6).

E. Wind Tunnel Model Design

The wind tunnel model has been designed to allow flexibility for testing not only the current circulation control concepts, but also adaptability to other flow control techniques in the future. The CFD studies presented above were used to supply estimated aerodynamic loads on all model components for the design and stress analysis. Figure 18 shows a view of the model mounted on the sidewall turntable, with the upper fuselage and upper wing skins removed. The model-mounting block in the center of the fuselage serves as the attachment to both the semi-span balance and the high-pressure air delivery bellows. The mounting block manifolds the high-pressure air into four independent flow paths, which are regulated by computer controlled ball valves mounted in the fuselage. The four supply lines are then routed through the wing box to supply four plenums in the trailing edge region. Although not discernable in this view, each plenum uses a stainless steel perforated choke plate to maintain the desired internal flow conditions. Although the CFD studies to date have not examined the spanwise variability of the blowing rate it is anticipated to be a useful feature of this model; for example, the ability to manipulate the spanwise distribution of lift or to provide roll control capability from the outboard plenum.

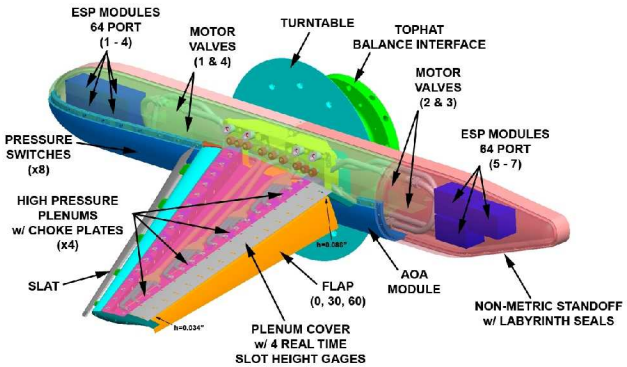

Figure 18. View of wind tunnel model in low-speed high-lift configuration.

The semi-span model is offset from the wind tunnel sidewall using a 2.0-inch non-metric standoff that is mounted to the turntable plate. A nominal 0.25-inch gap is maintained between the standoff and semi-fuselage and a labyrinth type flow blocker[17] is used to minimize the flow between the model parts. A multi-segment fouling circuit is used to monitor the behavior of the gap during testing. A small gap is also provided between the back of the standoff and wind tunnel wall, and a spring-loaded Teflon strip is used as a scrubbing flow blocker[17].

The design of the wing structure allows every component to be replaced except for the lower wing skin, which is integral to the wing box. In anticipation of testing leading edge flow control devices, the front spar has milled passageways for the routing of high-pressure air. Figure 19 shows the outboard portion of the wing in the high-lift mode, with the slat and 60° trailing edge flap installed. The plenum cover plate has been removed to highlight the airfoil shaped standoffs used to support the cover plate, and maintain the blowing slot height. Several non-intrusive variable capacitance gauges[23] will be installed in this region to monitor the behavior of the slot height during testing.

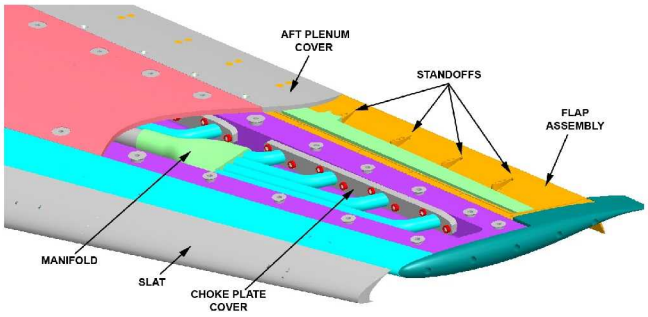

Figure 19. Detail view of wind tunnel model outboard wing in the low-speed high-lift configuration.

The model will be instrumented with four rows of pressure taps on the wing, shown in Figure 20 for the cruise configuration. In the high-lift mode, the slat and flaps will include pressure taps at these locations, as well as pressure taps inside the plenum to help characterize the internal flow exiting the blowing slot. The fuselage will have a row of pressure taps near the centerline, as well as one radial row ahead of the wing. The model has approximately 250 pressure taps. Electronically scanned pressure modules are housed in the nose and tail regions of the fuselage. The performance of the four plenums will be documented using several pressure measurements. Additional instrumentation housed in the fuselage includes the redundant model over-pressurization safety switches, and the model angle-of-attack inclinometer.

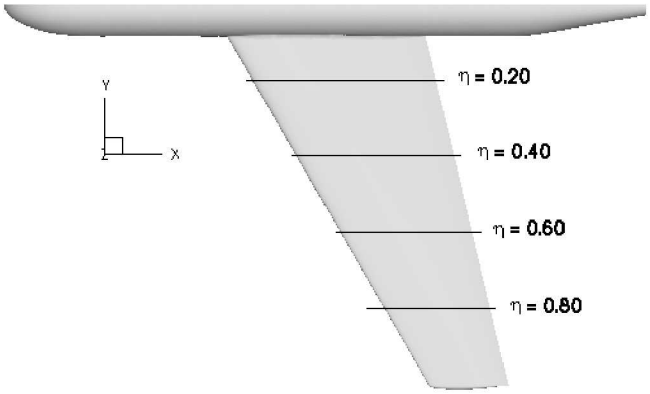

Figure 20. Location of pressure tap rows on cruise wing configuration.

F. NTF-117S Balance

The semi-span model test technique at the NTF has traditionally focused on high-Reynolds number testing of low-speed high-lift configurations. The NTF-114S balance used for this testing is not well suited for transonic testing due to the elevated model loads generated. A larger load capacity balance, the NTF-117S was fabricated in the late 1990s but not completed. As part of the current research program this balance was recently instrumented and calibrated. The new balance is shown in Figure 21, along with the various load capacities referenced to the balance moment center. The normal force capability of 12,000 lb is of particular interest for transonic testing. It is important to note that the physical dimensions of the new balance are identical to those of the NTF-114S balance, allowing either to be used with the new air station.

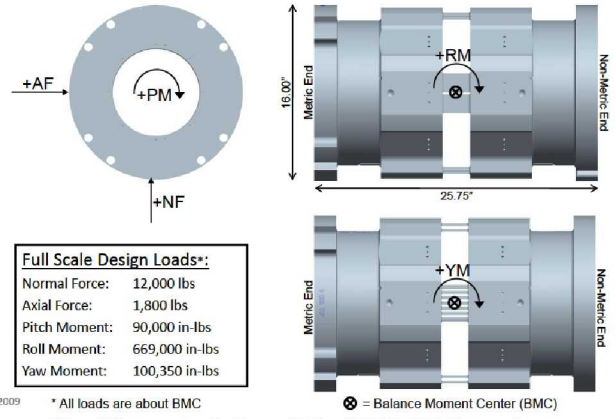

Figure 21. Characteristics of the NTF-117S semi-span balance.

The addition of the high-pressure air delivery supply lines and bellows do add more potential variables to the performance of the semi-span balance. Of particular interest are possible pressure tare and momentum tare interference effects. The engineering design analysis to date suggests that the bellows will have a minimal effect on the balance readings for two reasons: 1) the small size and relative stiffness of the bellows; and 2) the balance does not measure side force which is the anticipated direction of the predominate bellows forces. A second calibration of the NTF-117S is however currently being formulated to quantify the effects of the statically pressurized bellows on the balance accuracy. This calibration will be performed with the balance installed in the SMSS. To access the momentum tare effects, the check standard nozzle configuration discussed above will be used to examine the influence of the supply pressure and mass flow rate on the balance accuracy.

III. Concluding Remarks

The capability to test active flow control and propulsion simulations is being established in the National Transonic Facility at the NASA Langley Research Center, with capacity for high Reynolds number and Reynolds number effects testing. This testing technique is focused on the use of semi-span models due to their increased size and relative ease of routing high-pressure air to the model.

A new dual flow-path high-pressure air delivery station has been designed. The low mass flow leg of the air station is capable of delivery up to 8 lbm/sec of flow, while the high mass flow leg delivers up to 20 lbm/sec. The high-pressure air is routed through the sidewall mounting system, and through the center of the force and moment balance, connecting to the semi-span model with a co-flowing bellows arrangement. The wind tunnel models are protected by a model over-pressurization protection system, which is based on a series of fast acting isolation and ventilation valves. To avoid the formation of frost in the wind tunnel circuit the testing technique is limited to a minimum tunnel temperature of -50 $^{\circ}$F.

The first aerodynamic model to utilize the new air station is a high performance transonic wing model that was designed using state-of-the-art CFD methods. The wing will be used to examine various circulation control concepts at both transonic cruise, and at low-speed high-lift conditions. For the high-lift configuration, the circulation control blowing slot will be directed over a simple 15% chord hinged trailing edge flap, while the leading edge utilizes a conventional slat. The circulation control is applied via four independent plenums across the trailing edge of the wing, and supplied by four computer-controlled valves in the semi-fuselage. The model has been designed to allow testing of other active flow control techniques in the future.

Finally, a new semi-span force and moment balance has been completed and calibrated to allow testing at transonic Mach numbers. The new NTF-117S balance has a maximum normal force capacity of 12,000 lb. Plans have been formulated to access the interference tares imparted by the bellows, which will include the evaluation of the static pressure tares, as well as the momentum tares. The momentum tares will be evaluated using a series of Stratford calibration nozzles, mounted on a new check standard dual-nozzle model.

Acknowledgements

The authors would like to express their sincere gratitude to a large group of NASA and contract personnel who have contributed to this research effort. The scope of the project has required coordination with multiple organizations at the NASA Langley Research Center with a significant emphasis placed on the safe operation of the high-pressure air delivery station. The project has been supported by the Subsonic Fixed Wing project, with special thanks given to Mike Rogers and Richard Wahls, for their support and latitude in the execution of this new capability. The first author is grateful to Richard Campbell for his assistance in the use of the CDISC design method. The CFD computations were performed on the Columbia supercomputer at the NAS facility at NASA Ames Research Center.

The following individuals have played key roles in the design of the high-pressure air delivery station, and are recognized for their efforts and commitment to excellence: Bryan Haas and Mike Palmer for oversight of the air station design; Paul Smith for his detailed mechanical design for the SMSS modifications; Greg Gatlin for his shared expertise of the SMSS and semi-span model testing; Frank Beltinck and Jeremiah Berry for mechanical and electrical guidance inside the SMSS; Ray Rhew, Shirley Jones, and Chris Lynn for support of the NTF-117S balance

calibration activities; Dr. Balakrishna and Dave Butler for their preliminary design study and transient flow analysis, Bill Bissett and Arbria Wright for their support and leadership; and Mike Brewer and Steve Alperin who will oversee the air station construction and integration phase. The authors would also like to thank Larry Lake, Garry Grab, and Allan Sordelett of Progressive Design Inc. for their contributions to the air station design. The support and interest expressed by both Cale Zeune at the Air Force Research Lab, and Rick Hooker of Lockheed Martin are greatly appreciated. The authors also appreciate the continued interactions with Bob Englar, and his research staff at the Georgia Tech Research Institute.

References

[1] Gad-el-Hak, M, Pollard, A. Bonnet J (Ed), "*Flow Control – Fundamentals and Practices*", Springer, M 53, October 1997

[2] "*Guide for Verification and Validation of Computational Fluid Dynamics Simulations*", American Institute of Aeronautics and Astronautics, AIAA G-077, 1998.

[3] Roache, P.J., "*Verification and Validation in Computational Science and Engineering*," Hermosa Publications, 1998

[4] Jones, G.S., Joslin, R.D., "Proceedings of the 2004 NASA/ONR Circulation Control Workshop", NASA/CP-2005-213509, June 2005

[5] Jones, G. S., Yao, C., Allan, B.G., "Experimental Investigation of a 2-D Supercritical Circulation-Control airfoil Using Particle Image Velocimetry", AIAA-2006-3009, June 2006.

[6] Lin., J.C., Jones, G.S, Allan, B.G., Westra, B.W., Collins, S.W., and Zeune, C. H., "Flow-Field Measurement of a Hybrid Wing Body Model with Blown Flaps", AIAA Paper 2008-6718, July 2008.

[7] Jones, G.S., Viken, S.A., Washburn, A.E., Jenkins, L.N., & Cagle, C.M., "An Active Flow Circulation Controlled Flap Concept for General Aviation Applications", AIAA 2002-3157, June 2002.

[8] Englar, R. J., G. S. Jones, B. G. Allan, and J. C. Lin, "2-D Circulation Control Airfoil Benchmark Experiments Intended for CFD Code Validation," AIAA Paper 2009-0902, January 2009.

[9] Min, B.Y., Lee, W, Englar, R., and Sankar, L.N., "Numerical Investigation of Circulation Control Airfoils" *Journal of Aircraft*, Vol. 46, No. 4, 2009, pp. 1403 – 1410.

[10] Collins, S.W., Westra, B.W., Lin., J.C., Jones, G.S., and Zeune, C. H., "Wind Tunnel Testing of Powered Lift, All-Wing STOL Model", International Powered Lift Conference, Royal Aeronautical Society, London, July 2008.

[11] Englar, R. J., "Two- Dimensional Transonic Wind Tunnel Tests of Three 15-Percent –Thick Circulation Control Airfoils," Naval Ship R&D Center Technical Note AL-182, AD 882-075, Dec. 1970.

[12] Jones, G.S, Lin., J.C., Allan, B.G., Milholen II, W.E., Rumsey, C.L., and Swanson, R.C., "Overview of CFD Validation Experiments for Circulation Control Applications at NASA", International Powered Lift Conference, Royal Aeronautical Society, London, July 2008.

[13] Englar, R. J., G. S. Jones, B. G. Allan, and J. C. Lin, "2-D Circulation Control Airfoil Benchmark Experiments Intended for CFD Code Validation," AIAA Paper 2009-0902, January 2009.

[14] Swanson, R. C. and Rumsey, C. L., "Numerical Issues for Circulation Control Calculations," AIAA Paper 2006-3008, June 2006

[15] Pfingsten, K.C and Radespiel, R., "Experimental and Numerical Investigation of a Circulation Control Airfoil", AIAA 2009-533, January 2009

[16] Wetzel, D., Griffin, J., Liu, F., and Cattafesta, L., "An Experimental Study of Circulation Control on an Elliptic Airfoil", AIAA-2009-4280, June, 2009

[17] Gatlin, G.M, Tomek, W.G., Payne, F.M., and Griffiths, R.C., "Recent Improvements in Semi-Span Testing at the National Transonic Facility (Invited)", AIAA Paper 2006-508, January 2006.

[18] Barrier, B.L., Leavitt, L.D., and Bangert, L.S., "Operating Characteristics of the Multiple Critical Venturi System and Secondary Calibration Nozzles Used for Weight-Flow Measurements in the Langley 16-Foot Transonic Tunnel", NASA TM 86405, 1985.

[19] Frink, N. T., "Tetrahedral Unstructured Navier-Stokes Method for Turbulent Flows," *AIAA Journal*, Vol. 36, No. 11, November 1998, pp. 1975-1982.

[20] Campbell, Richard L, "Efficient Viscous Design of Realistic Aircraft Configurations (Invited)", AIAA Paper 98-2539, June 1998.

[21] Milholen, II, W.E., and Owens, L.R., "On the Application of Contour Bumps for Transonic Drag Reduction (Invited)", AIAA Paper 2005-0462, January 2005.

[22] Englar, Robert J., et al.,"Experimental Development of CC airfoils and Pneumatic Powered-Lift Systems," AIAA 2010-0345, January 2010.

[23] Manning, B., Doussin, J.F., "Best Practices in the use of "Smart" Displacement, Gap and Hole Mapping Sensors for Aircraft and Aircraft Engine test and overhaul", Aerospace Texting Expo 2005, Hamburg, Germany, *April 6, 2005*